Macromolecular Research, Vol. 13, No. 5, pp 418-426 (2005)

One-Pack Cross-linkable Waterborne Methyl Ethyl Ketoxime-Blocked Polyurethane/Clay Nanocomposite Dispersions

Sankaraiah Subramani, Jung Min Lee, and Jung Hyun Kim

Department of Chemical Engineering, Yonsei University, Seoul 120-749, Korea

In Woo Cheong*

Department of Applied Chemistry, Kyungpook National University, Daegu 702-701, Korea

Received July 7, 2005; Revised October 5, 2005

Abstract: One-pack cross-linkable nanocomposites of waterborne methyl ethyl ketoxime (MEKO)-blocked aromatic polyurethane dispersion (BPUD) reinforced with organoclay (quaternary ammonium salt of Cloisite 25A) were synthesized by the acetone process using 4,4′-methylenedi-*p*-phenyl diisocyanate (MDI), poly(tetramethylene) glycol (PTMG), dimethylol propionic acid (DMPA), and methyl ethyl ketoxime (MEKO). Particle size, viscosity, and storage stability of these nanocomposites were investigated. TEM and XRD studies confirmed that the silicate layers of organophilic clay were exfoliated and intercalated at a nanometer-scale in the BPUD matrix.

Keywords: polyaddition, waterborne, polyurethane, dispersions, nanocomposite, morphology, blocked polyurethane.

Introduction

Nanocomposites are a new class of composite material, which can be defined as the distribution of a second (or even third) phase of nanometric dimension in a matrix that can be amorphous or crystalline. Polymer nanocomposites are generally defined as the combination of a polymer matrix resin and inorganic particles, which have at least one dimension (i.e. length, width, or thickness) in the nanometer size range. In polymer nanocomposites, fillers have important roles in the modification of polymer properties. Effects of fillers on the properties of nanocomposite depend on their concentration, particle size, and shape as well as on the interaction with the matrix. Inorganic particles such as, clay, SiO_2, and TiO_2 are widely used as reinforcement materials for host polymers. Among these inorganic materials, clay has been receiving special attention in the field of nanocomposites because of its sub-micron particle size and intercalation properties. After the development of Nylon/montmorillonite nanocomposite,[1-3] a large number of new polymer nanocomposites have been investigated.[4-12] Most of the polymer/clay nanocomposites were almost based on glassy polymers with high glass-transition temperatures, such as PMMA, PS, SAN, and epoxy, however, studies of rubbery polymers have rarely been reported.

Polyurethanes (PUs) are noted as versatile polymeric materials, which can be tailored to meet the highly diversified demands of modern technologies such as coatings, adhesives, reaction injection molding, fibers, foams, rubbers, thermoplastic elastomers, and composites.[13-15] Properties of PU are modified either by varying PU microstructure, resulting from step-growth polymerization of isocyanate resins with polyols, or by dispersing inorganic and organic fillers within the PU continuous matrix. Recently, research work related to PUs has been oriented towards improving mechanical properties including solvent, water, scratch, and abrasion resistance properties. A wide variety of fillers, including clay and wollastonites, is being applied in PU formulations to reduce costs and to reinforce the PU matrix.[16] Properties of filled PUs are dependent upon filler shape, average diameter, and interfacial coupling. Many patents and papers describe the synthesis, properties and usage of special organophilic clays in PU nanocomposites.[17-27] However, only few studies have been reported about the aqueous aliphatic PU nanocomposites,[28-30] There is no scientific literature which dealt with nanocomposites from blocked aromatic polyurethane (BPUD)/organophilic clay.

In the present study, it is firstly aimed to improve the properties of the aromatic BPUD by reinforcing PU with organically modified clay. The objective of this research is synthesis and characterization of one-pack cross-linkable BPUD/organophilic clay nanocomposite by dispersing the nanometer-scale silicate layers into the BPU.

*Corresponding Author. E-mail: inwoo@knu.ac.kr

Experimental

Materials. All raw materials are laboratory grade chemicals and were used as received. Poly(tetramethylene) glycol (PTMG; 1,000 g/mol) was dried in vacuum at 80 °C for 6 hrs before use. Dimethylol propionic acid (DMPA) was dried at 50 °C for 24 hrs in a vacuum oven. *N*-methyl-2-pyrrolidone (NMP) and acetone were stored over well-dried molecular sieves. 4,4′-methylenedi-*p*-phenyl diisocyanate (MDI), methyl ethyl ketoxime (MEKO), triethylamine (TEA), phenylamino propyl trimethoxy silane (PAPTMS), and tetraethylene pentamine (TEPA) were used as received. Organoclay, Cloisite 25A, was dried at 60 °C for 12 hrs under vacuum. In this organoclay, the cations of natural montmorillonite were replaced by dimethyl, hydrogenated tallow and 2-ethylhexyl quaternary ammonium ions. The weight loss on ignition is 34% and the modifier concentration is 95 meq/100 g of clay. Distilled and deionized (DI) water was used.

Synthesis of Waterborne MEKO-blocked PUD/Clay Nanocomposite. A 500 mL rounded, four-necked separable flask with a mechanical stirrer, nitrogen inlet, thermometer, and condenser was charged with 15.00 g PTMG and different concentration of Cloisite 25A(BI0~BI5 in Table I, 0, 1.0, 3.0, and 5.0 wt% based on total solid). The reaction was performed in a thermostat with agitation for 5 hrs at 75 °C for the exfoliation of Cloisite 25A by PTMG. To the above PTMG/Cloisite 25A mixture, 1.34 g DMPA dissolved in 2.68 g NMP was added and the reaction mixture was further stirred at 75 °C for 2 hrs under N_2 atmosphere. After mixing, 10.01 g MDI was added to the reaction mixture and the reaction was allowed for 1 hr to obtain NCO-terminated prepolymer. Then the reaction temperature was reduced to 50 °C and 15.00 g acetone was added to reduce the viscosity of the NCO-terminated prepolymer. To obtain blocked PU prepolymer, 2.61 g MEKO was slowly added for 0.5 hrs. The reaction was carried out until NCO peak disappeared in the FTIR spectrum and then 1.01 g TEA was added and allowed to react for 0.5 hrs. At the end of the reaction, calculated amount of DI water was added to accomplish the dispersion under vigorous stirring. Uniform and stable dispersion was obtained, from which the acetone was removed under reduced pressure at 50 °C. The solid content of the resulting dispersion was adjusted to 30 wt%. All the experiments were carried out without catalyst to avoid side reactions.

Table I. Physical Properties of Waterborne BPUD/Clay Nanocomposites

Properties \ Sample ID		BI0	BI1	BI3	BI5
Cloisite 25A (wt%)		0	1.0	3.0	5.0
$\overline{D_n}$ (nm)		67	85	113	137
Viscosity (cps)		24	21	19	11
De-blocking Temp (°C)		90-200	-	-	115-200
Storage Stability (months)	at RT	> 6	> 6	> 6	> 6
	at 60 °C	> 1	> 1	> 1	> 1

In the above prepared BPUD/organoclay nanocomposites, the cross-linkers, PAPTMS and TEPA aqueous solutions, were added in stoichiometric amounts based on the isocyanate content to cross-link the BPUD/organoclay nanocomposites to make one-pack cross-linked waterborne nanocomposites, BI0-S~BI5-S and BI0-T~BI5-T with PAPTMS and TEPA, respectively (see Table II).

Film Formation and Cross-linking. The BPUD/organoclay nanocomposites containing well-dispersed cross-linkers (PAPTMS or TEPA) were cast on a silicone trough and water was allowed to evaporate at room temperature. The remaining moisture was removed under vacuum at room temperature for 6 hrs. Dried nanocomposites films were deblocked to investigate an effect of cross-linking in an air-

Table II. Nano-indentation Data and Tensile Properties of BPUD/Organoclay Nanocomposite Films Cross-linked with PAPTMS and TEPA

Samples	Load[a] (mN)	Depth[a] $\times 10^{-4}$(nm)	Modulus[a] $\times 10^{2}$(GPa)	Hardness[a] $\times 10^{3}$(GPa)	Tensile[b] Strength (MPa)	Elongation[b] (%)
BI0-S	39.7	2.2	7.9	5.0	16.0	185
BI1-S	41.6	1.8	14.5	7.2	22.3	175
BI3-S	46.5	2.2	9.3	5.5	20.5	155
BI5-S	47.1	1.7	15.2	8.8	19.0	45
BI0-T	36.9	2.9	3.5	2.8	8.3	246
BI1-T	39.6	2.2	7.2	5.1	10.2	232
BI3-T	40.1	2.5	4.9	5.5	11.9	220
BI5-T	42.4	1.9	10.3	7.1	12.5	212

[a]Measured by Nano-indentation method. [b]Measured by UTM.

circulating oven at 125 °C. After 30 min of baking, the films were removed from the oven and kept at room temperature for one week to effect moisture cross-linking of the terminal alkoxysilane (methoxy silane) groups (in the case of PAPTMS). The cross-linked films were well dried in a vacuum oven and taken for characterization.

Characterizations. The average particle size ($\overline{D_n}$) and viscosity of the waterborne BPUD/organoclay nanocomposites were measured using a BI-particle sizer ZPA (Brookhaven Inst. Co.) and Brookfield LVDV-II viscometer, respectively, at 25 °C. The BPUD/organoclay nanocomposites in a sealed bottle were kept in a convection oven at 60 °C to examine their storage stability.

X-ray diffraction (XRD) experiments were performed directly on the film samples using a X-ray diffractometer (Rigaku D/max-Rint 2000) at 30 kV and 20 mA with Cu Kα radiation source (λ=1.5404 Å) at a scan speed of 4° min^{-1} in the range of 1~60°. Nanocomposites samples were measured as films with 0.1-0.3 mm thickness.

The samples for transmission electron microscopy (TEM, JEOL 1200EX) study were first prepared by putting cross-linked BPUD/organoclay nanocomposite films into epoxy capsules and curing the epoxy at 70 °C for 24 hrs in a vacuum oven. Then the cured epoxies containing cross-linked BPUD/organoclay nanocomposite were microtomed with cryogenic ultramicrotome system by a diamond knife into 50 nm-thick slices in a direction normal to the plane of the films, and then placed on 200-mesh copper grids for TEM.[31]

Dynamic mechanical properties were determined using a dynamic mechanical thermal analyzer (Rheometry Scientific DMTA MK III) with a tensile mode. The samples were cooled to −100 °C, equilibrated for 3 min at this temperature, and then heated to 150 °C at a constant heating rate of 5 °Cmin^{-1} at a frequency of 10 Hz under N_2 atmosphere.

A nano-indentation tester (MTS XP System with diamond Berkovich type indenter tip) was used to measure the mechanical properties of the nanocomposite films. Multiple indentations were made at different locations of the film surface at a fixed applied load. The load-displacement curve was recorded, from which the effective hardness and modulus could be calculated.

Tensile properties of the dispersion-cast films were measured using a universal tensile machine (INSTRON) at a crosshead speed of 0.1 m min^{-1}. Sample specimens were prepared from the films with a die of dimension of 10 mm width and 40 mm length, the grip distance was set at 20 mm. Thickness of the film was 0.10-0.30 mm. For each film three specimens were tested and the average value was reported.

Differential scanning calorimeter (DSC, TA Instruments Model DSC Q10) was used to examine both de-blocking temperature and glass transition temperature (T_g) of the nanocomposite samples with a heating rate of 10 °C min^{-1} under nitrogen purge of 30 mL min^{-1}. The sample size was 3-10 mg in a sealed aluminum pan. Thermo-gravimetric analysis (TGA, TA Instr., TGA Q50) was carried out with sample weight of 3-10 mg. The experimental run was performed from 30 to 600 °C at a heating rate of 20 °C min^{-1} in nitrogen atmosphere with a gas flow rate of 30 mL min^{-1}.

The water and xylene resistances of the films were tested as follows: A pre-weighed dry slabs (5×5 mm in size) were immersed in deionized water to study water resistance and in xylene to study xylene resistance at 25 °C. After immersing, the samples were blotted with a laboratory tissue and weighed. The swelling ratio (water uptake) was expressed as the weight percentage of water in the swollen sample:

$$\text{Swelling ratio} = (W_S - W_D)/W_D \times 100(\%) \quad (1)$$

where, W_D is weight of the dry sample and W_S is the weight of the swollen sample. Transparency was measured with UV-visible spectrophotometer (HITACHI U-2010) using a film with 0.3 mm thickness.

The gel content was calculated as follows: A sample of approximately 0.1 g (w_1) was wrapped in 300-mesh stainless steel mesh of known mass (w_2) and exposed to 100 mL of xylene at 100 °C for 24 hrs. The stainless steel mesh was then removed and the mass was measured after vacuum drying at 80 °C for 24 hrs (w_3). The degree of cross-linking was measured in terms of the percent gel content, using the equation:

$$\text{Gel content (\%)} = \{(w_3 - w_2)/w_1\} \times 100(\%) \quad (2)$$

Results and Discussion

In the BPUD/organoclay nanocomposite dispersions, the organoclay 'swells' (i.e. its layers are separated by hydration[32]) which makes its good dispersion in the PU possible. The dispersion prepared by adding 7.0 wt% of clay was not stable and settling of clay was observed after 2 days of preparation, which was due to the high solid content of the resulting nanocomposite dispersion, poor wetting and high density of organoclay. This shows that there is a limitation in clay loading in waterborne systems to make respective nanocomposites.

Particle Size and Viscosity of BPU/Organoclay Dispersions. The physical properties of BPUD/organoclay nanocomposite dispersions were presented in Table I. In general, $\overline{D_n}$ of PUD depends on many factors such as type and content of isocyanate, polyols, DMPA (hydrophilicity), blocking agent, and degree of neutralization. In these experiments equimolar amount of TEA based on DMPA content was used with different amount of organoclay. The $\overline{D_n}$ increased as the content of organoclay increased, which may be due to the charge neutralization effect of anionic charge from DMPA by the quaternary ammonium salt of organoclay. Another probable reason can be the residual aggregates of quaternized organoclay in the aqueous phase, which

increases of ionic strength of aqueous phase to suppress the thickness of electrical double layer of the anonically stabilized BPU particles.

The viscosity of BPUD/organoclay nanocomposites decreased as the content of clay increased. In general the viscosity of aqueous dispersion is inversely proportional to the particle size,[33] which is attributed to the smaller total effective volume of larger particle. In addition, the viscosity decreases when the electro-viscosity effect (the change in viscosity due to the presence of charge on particles dispersed in a solvent) decreases, which is probably due to the addition of quaternized organoclay as mentioned above.

Storage studies were performed at two conditions, i.e., room temperature (25 °C) for six months and 60 °C for one month, respectively, to evaluate the storage stability of dispersions and the results are given in Table I. The data reflect that all dispersions were stable and the stability clearly indicated that the de-blocking of the BPUD does not occur in the dispersion.

Morphology of BPUD/Organoclay Nanocomposite Films. XRD patterns for the organoclay as well as for the nanocomposite films are presented in Figure 1(A) and 1(B). A peak at 2θ=4.8° was observed in the XRD of organophilic clay. However, there was no distinguishable peak could be observed in the XRD of the BPUD/organoclay nanocomposite films when the organophilic content were 1.0, 3.0, and 5.0 wt%. This indicated that almost all the silicate layers dispersed in nanometer-scale in the BPU matrix lost their crystallographic ordering due to exfoliation and intercalation, which generally depends on the molecular weight of the resulting BPU polymer and surface wetting of the organoclay.

Typical TEM images of BI3-S and BI5-S BPUD/organoclay nanocomposite films are shown in Figure 2A and 2B, respectively. Since the silicate layers are composed of heavier elements (Al, Si, O) than the interlayer and surrounding matrix (C, H, N), they appear darker in bright field images.[34] The dark lines correspond to the individual silicate platelets in the BPU matrix. Some single silicate layers and ordered intercalated assembled layers of clay are well dispersed in the BPU matrix. On the basis of the aforementioned TEM and XRD results, the BPUD/organoclay dispersion samples were apparently a nanocomposite with the intercalated or exfoliated structures of clay. The low magnification view in Figure 2A(a) and 2B(a) show that the clay is well dispersed in the BPU matrix. Figure 2A(b) and 2B (b) show a higher magnification picture, which reveals that clay is intercalated and exfoliated in the PU matrix with layer distances of 1–10 nm. The dark lines in Figure 2A(b) and 2B(b) are the cross-sections of single or possibly multiple silicate platelets. The platelets are flexible and, thus, show some curvature. This result confirmed that the layered silicates were mostly intercalated in the BPU nanocomposites, and the individual silicate layers in BI3-S and BI5-S were far less separated. The average thickness of the clay platelets appears to be approximately 2 nm.

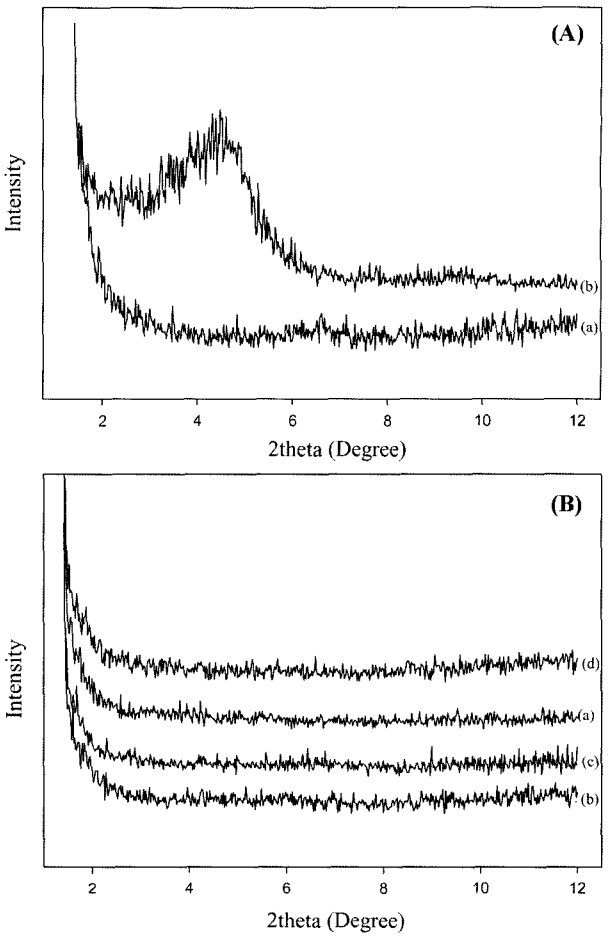

Figure 1. (A): XRD patterns of (a) BI5-T nanocomposite film and (b) organoclay. (B): XRD patterns of (a) BI0-S, (b) BI1-S, (c) BI3-S, and (d) BI5-S nanocomposite films.

Nano-indentation and Tensile Properties. The modulus and hardness of a polymeric film mostly depend on the cross-linking density of the nanocomposite films and filler loading/reinforcement effect. The changes in the depth, modulus and hardness with an applied load of nanocomposite films were summarized in Table II. As seen in Table III, with an applied load (target load 50,000 μN), the penetration decreased in the order: BI0-S > BI1-S > BI3-S > BI5-S and both modulus and the hardness increased in the order: BI0-S < BI1-S < BI3-S < BI5-S.

In the case of the TEPA cross-linked nanocomposites, the same trend was observed and this again confirms the enhancement of mechanical properties with increase in clay content and reinforcing effect by the intercalation or exfoliation of the silicate layers. The nanocomposite films obtained from PAPTMS show higher modulus and hardness compared to TEPA cross-linked ones. This might be due to the higher cross-linking density of the PAPTMS film and it was

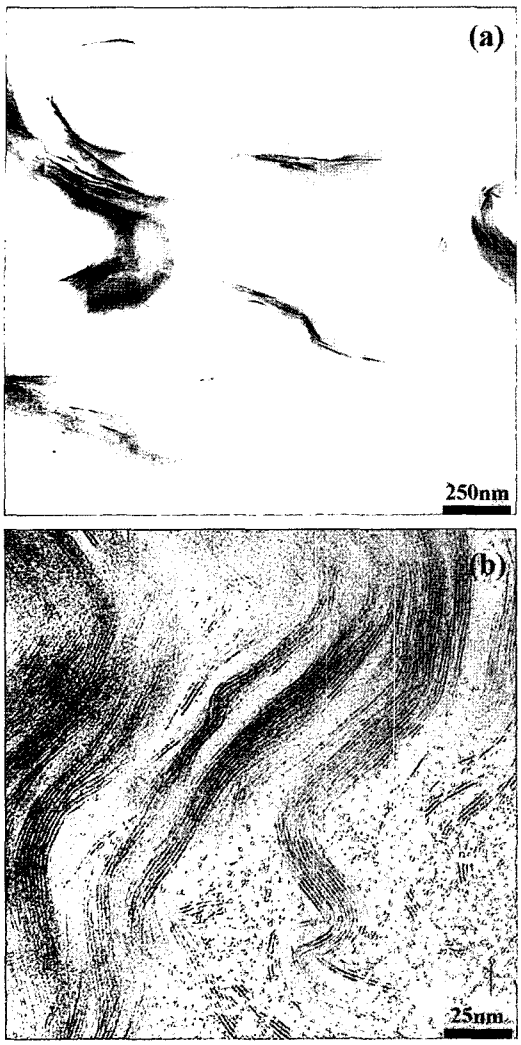

Figure 2A. TEM images of BI3-S. Scale bars (a) 250 nm at ×10 K and (b) 25 nm at ×100 K magnifications.

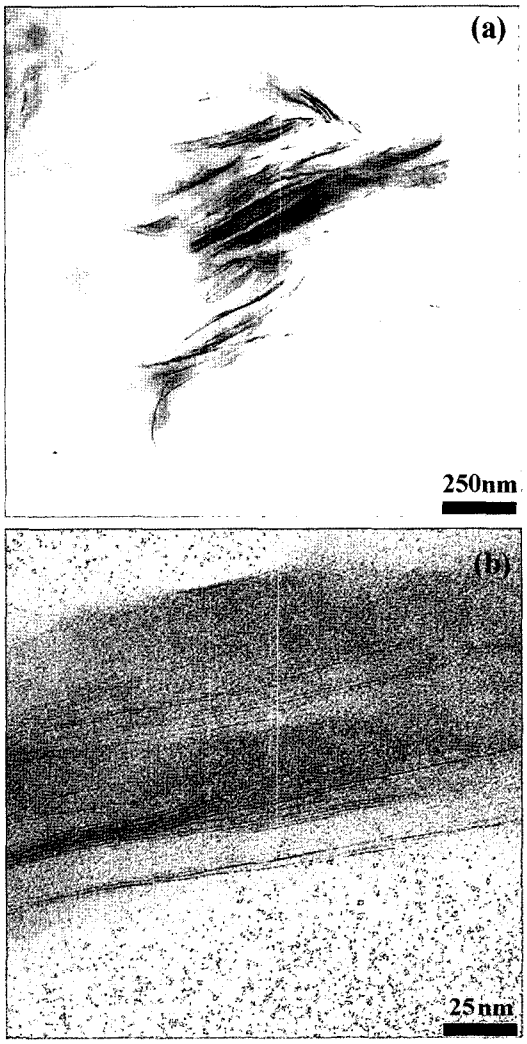

Figure 2B. TEM images of BI5-S. Scale bars (a) 250 nm at ×10 K and (b) 25 nm at ×100 K magnifications.

further confirmed by gel content test. The gel content for PAPTMS films is 87.1% whereas it is 82.4% for TEPA-based films. The enhancement of the modulus was ascribed to the resistance exerted by the clay itself, as well as the orientation and high aspect ratio of the clay platelets.[35]

The tensile properties of the films were measured and presented in Table II. In this test, BPUD/organoclay nanocomposites containing PAPTMS (from BI0-S to BI5-S) or TEPA (from BI0-T to BI5-T) are de-blocked to regenerate the NCO groups and the regenerated NCO groups react further with PAPTMS or TEPA to form cross-linked BPU/clay nanocomposite films. It can be seen that the tensile strength increases and elongation at break decreases as the organoclay content increases in both sets of nanocomposites, PAPTMS and TEPA as expected and the improvement in the tensile strength of the nanocomposites indicates that the strong interfacial interaction between the silicate surface and the nearby polymer chains.[36] Between the PAPTMS and TEPA

Table III. Glass Transition Temperatures and Transmittance of Nanocomposites Films (BI0-S ~ BI5-S and BI0-T ~ BI5-T)

Samples	T_g (°C) (Soft Segment)	Transmittance (%)		
		633 nm	514 nm	488 nm
BI0-125°C	-21.1[a]	-	-	-
BI5-125°C	-23.0[a]	-	-	-
BI0-S	-	70.9	64.6	59.5
BI1-S	-	70.8	66.7	64.4
BI3-S	-	67.1	60.1	57.7
BI5-S	-	60	58.2	57.0
BI0-T	-10[b]	67.4	66.9	64.4
BI1-T	-10[b]	65.3	59.5	58.0
BI3-T	-	63.7	62.4	55.9
BI5-T	-	60.5	59.1	58.3

[a]Measured by DSC. [b]Measured by DMTA.

cross-linked nanocomposites, PAPTMS cross-linked BPU/clay nanocomposite films exhibit higher tensile properties compared to TEPA cross-linked ones, which probably may due to the different layer structure of intercalated and exfoliated silicates between the soft and hard segments arising from the different cross-linking densities by respective cross-linkers as mentioned before.

Dynamic Mechanical Properties. Figures 3 and 4 show the dynamic mechanical properties of the two types of nanocomposite films. It was seen from the Figure 3 that storage modulus (E') increases marginally with an increase in the content of organoclay in both sets of nanocomposite films. For all nanocomposite films, the large drops of tensile storage modulus, E', occur on heating at the T_g's of soft segment and hard segment domains. The improvement of E' by added clay is marginal at the temperature range below the T_g of hard domain. However, the presence of clay evidently enhances the E' values to develop rubbery plateau at the temperature range above the T_g of hard segment domain. The strong confining effect of the silicate layers on the movement of the intercalated PU molecule existing in the two-dimensional host galleries seems to prohibit the flow of PU molecule and sustain the rubbery state even at the temperature range above the T_g of hard-segment domain. In epoxy-clay nanocomposite, the improvement of tensile modulus and tensile strength also was more evidently observed at the temperature range above T_g compared with those below T_g.[37] This evident improvement at the temperature range above T_g was explained by the enhanced shear deformation and stress transfer to the platelet particles due to the increased elasticity of the matrix at the temperature range above T_g.[37] When the matrix polymer is in a glassy state, even though silicate layers are ceramic in nature, because of their very large aspect ratio and nanometer thickness, they may behave mechanically more like flexible sheets of paper than rigid plates.[38] This might explain the marginal improvement of E' by added clay at the temperature range below the T_g of soft segment.

Figure 4 of tan(δ) peaks shows single damping peak around 40-75 °C, which indicates that PAPTMS cross-linked nanocomposite films have phase-mixed morphology, and it may be the glass transition temperature of hard/soft segment mixed phase of PU polymer. The microphase miscibility of soft and hard segments of these BPUD/organoclay nanocomposite films is likely due to the relatively low molecular weight of the polyol.[39] Since the BPU nanocomposite films show phase-mixed morphology (single transition) and consequently do not crystallize, it is expected that the mechanical properties are mainly governed by the clay loading and cross-linking density. Unlike PAPTMS, TEPA cross-linked nanocomposites (BI1-T in Figure 4) show two broad damping peaks around -10 and 110 °C, which may be the glass transition temperature of soft segment-rich and hard segment-rich phase of PU polymer, respectively, and these

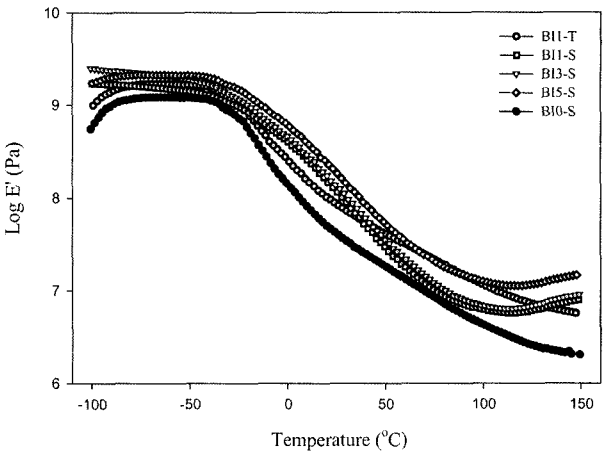

Figure 3. Storage modulus of the nanocomposite films (BI0-S ~ BI5-S and BI1-T).

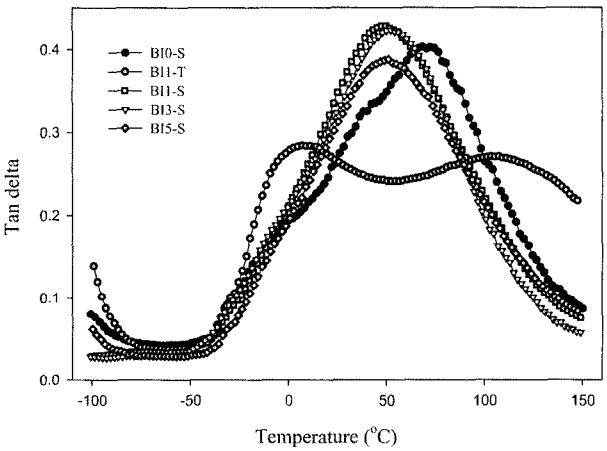

Figure 4. Tan δ of the nanocomposite films (BI0-S ~ BI5-S and BI1-T).

indicate the phase-separated morphology. Higher T_g of TEPA cross-linked nanocomposite films compared to pure PTMG (-88 °C)[40] suggests that there are partial phase mixing between soft and hard segments. The transition of the peaks varies slightly in nanocomposite films of the both types. This confirms the phase mixing between soft and hard segments and it varies in the presence of clay.

DSC and TGA Studies. The de-blocking behavior and thermal properties of the pure BPUD/organoclay nanocomposites and cross-linked (by PAPTMS and TEPA) nanocomposite films were studied by DSC, and the results are presented in Table III and Figures 5-6. From Figure 5, it can be seen that the BPUDs containing clay (0 and 5.0 wt%) are de-blocked around 110-120 °C. This result was confirmed by our previous publications[41] and it was noted that the de-blocking temperature was not affected by addition small amount of clay.

The T_gs of the pure BPUD/organoclay nanocomposites

(BI0 and BI5) baked at 125 °C are -21.1 and -23 °C, respectively, as shown in Table III and Figure 6. The T_g of the cross-linked nanocomposite films was unable to detect from DSC scans and it is probably because the transition extends over a wide interval due to cross-linking. The glass transition indicates the movement of polymer backbone, however, in the cross-linked network these movements are arrested and hence the T_g of the polymers were indiscernible. In addition, it was reported that the effect of small amounts of dispersed silicate layers on the free volume of PU is insignificant to influence the glass transition temperature of BPU/clay nanocomposites.[32]

The TGA curves of the pure BPUD/organoclay nanocomposites and cross-linked (PAPTMS and TEPA) nanocomposite films are shown in Figures 7 and 8. The de-blocking temperatures of nanocomposite films are given in Table I. The blocked PUs having 0 and 5.0 wt% clay are found de-blocked around 90 and 115 °C, respectively. The de-blocking temperature measured by DSC technique was slightly higher than TGA technique. The de-blocking temperature was influenced slightly by the addition of small amount of clay and it was reported that inorganic oxide pigments (fillers) have very little influence on the de-blocking temperatures of blocked isocyanate adducts.[42] The thermal degradation temperatures of the nanocomposites also increased very little compared to that of the pure BPUD/organoclay nanocomposites (BI0-S and BI0-T). It is generally believed that the introduction of inorganic components into organic materials can enhance their thermal resistance, as the dispersed silicate layers hinder the permeability of volatile degradation products out of the material.[36,43] Among the cross-linkers, PAPTMS cross-linked nanocomposite films show higher thermal stability with compared to those of TEPA cross-linked ones. This might be due to the higher cross-linking density of the PAPTMS films and high thermal stability of siloxane (-Si-O-Si-) network. In addition, thermal resistance increases with an increase in the clay content.

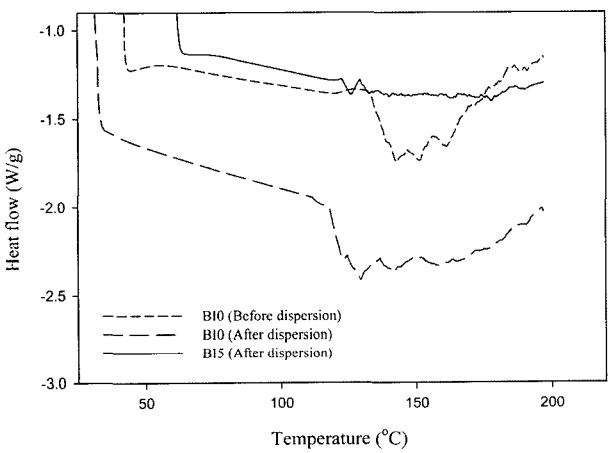

Figure 5. DSC curves of MEKO-BPUD/organoclay nanocomposite films (BI0 and BI5).

Swelling and Transparency Studies. Water and xylene resistances of the nanocomposite films were tested and % swelling was tabulated in Table IV. The % water absorption values of the films containing 1.0, 3.0, and 5.0 wt% clay were lower than those of pure BPU and nanocomposite film containing 0% clay. This could be due the presence of dispersed impermeable silicate layers in the PU matrix, which reduces the water swell and enhances the water resistance.[29] It was also reported that when the addition of organoclay (treated with 12-aminolauric acid or benzidine) became more than 1%, the water absorption function of clay became dominant leading to slight higher water absorption.[32] In the case of xylene, the solvent resistance shows marginal difference with pure nanocomposite film. Both water and xylene resistances of PAPTMS cross-linked nanocomposite films were superior to those of TEPA cross-linked films, which should be closely related to cross-linking density difference. Based on the above results, one can confirm that the organic

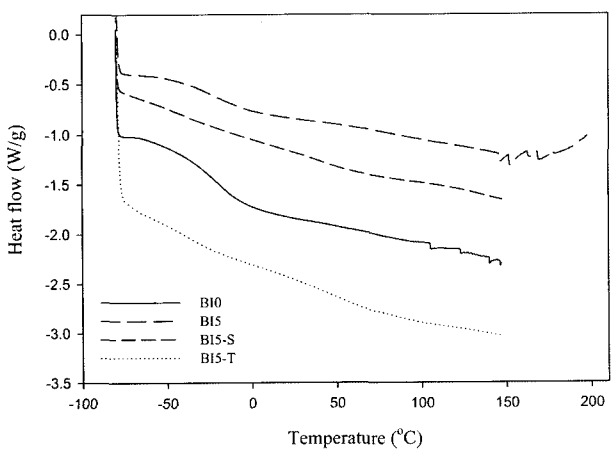

Figure 6. DSC curves of pure and cross-linked BPUD/organoclay nanocomposite films (BI0, BI5, BI5-S and BI5-T).

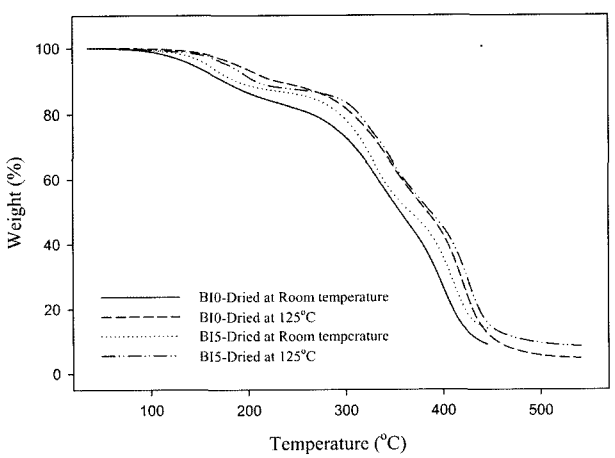

Figure 7. TGA curves of the MEKO-BPU/clay nanocomposite films (BI0 and BI5).

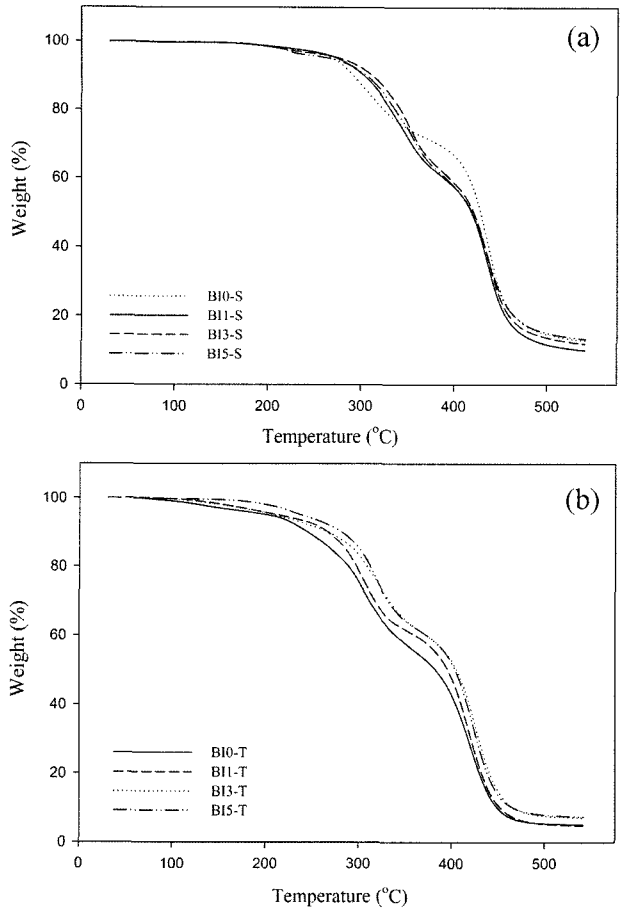

Figure 8. (a) TGA thermograms of the PAPTMS-based nanocomposite films (BI0-S~BI5-S). (b) TGA thermograms of the TEPA-based nanocomposite films (BI0-T~BI5-T).

modifiers have some effect on the water and solvent resistances of nanocomposite. The enhancement in the water and solvent resistances of the nanocomposite might also be due the intercalation and exfoliation of organoclay and depends on the hydrophobicity of treated clay.

Transparency of the BPUD/organoclay nanocomposite films were measured and presented in Table III. As shown in Table III, the transparency was not affected (i.e., reduced) so much by the addition of very small amount organoclay,[44] because its layer thickness is less than the wavelength of visible light. As like water and solvent resistance, transparency is also an important property for many applications in coatings and films, especially for the water based polymer systems.

Conclusions

One-pack cross-linkable waterborne MEKO-blocked PUD/organophilic clay nanocomposite dispersions were prepared and investigated in terms of cross-linking effect by using different cross-linkers, i.e., PAPTMS and TEPA. The TEM and XRD studies confirmed that morphology of the nanometer-scale silicate layers of organophilic clay were intercalated and exfoliated in PU matrix.

The modulus, tensile strength and hardness were enhanced by the reinforcing effect of intercalated and exfoliated organophilic clay and increased as the content of clay increased.

Higher modulus, tensile strength, hardness and lower percentage elongation of PAPTMS cross-linked films compared to TEPA cross-linked ones confirmed that PAPTMS cross-linked nanocomposite films were well cross-linked. Thermal stability, water and xylene resistances of the nanocomposites were enhanced compared to the pure BPU and these properties increased further with clay content that are dispersed in nanometer-scale.

Thermal, water and xylene resistance of the PAPTMS cross-linked films were higher than those of TEPA based nanocomposites.

Transparency of the films was not much affected by addition of organically modified clay.

Table IV. Water/Xylene Swelling and Gel Content of the BI5 and Nanocomposite Films (BI0-S~BI5-S and BI0-T~BI5-T)

Dispersion Sample	Water Swell (%) after			Xylene Swell (%) in 24 hrs	Gel Content (%)
	1 day	3 days	5 days		
Pure BI5	51.4	74.3	77.1	Disintegrated	-
BI0-S	5.9	5.9	5.9	47.1	87.1
BI1-S	5.0	5.0	5.0	45.5	-
BI3-S	3.9	3.9	4.8	47.6	-
BI5-S	1.5	2.9	4.4	46.7	-
BI0-T	11.1	16.7	16.7	57.1	82.4
BI1-T	7.7	15.4	15.4	58.8	-
BI3-T	5.6	11.1	11.1	61.1	-
BI5-T	4.4	5.9	11.8	60	-

Acknowledgements. S Subramani gratefully acknowledges the award of an International Fellowship of Yonsei University.

References

(1) Usuki, *et al.*, US Patent 4889885 (1989).
(2) A. Okada, T. Usuki, T. Kurauchi, and O. Kamigaito, *ACS Symposium Series*, **585**, 55 (1995).
(3) Y. Kojima, A. Usuki, M. Kawasumi, A. Okada, T. Kurauchi, and O. Kamigaito, *J. Polym. Sci.; Part A: Polym. Chem.*, **31**, 1755 (1993).
(4) M. S. Wang and T. J. Pinnavaia, *Chem. Mater.*, **6**, 48 (1994).
(5) P. B. Messersmith and E. P. Giannelis, *Chem. Mater.*, **6**, 1719 (1994).
(6) T. Lan, P. D. Kaviratna, and T. J. Pinnavaia, *Chem. Mater.*, **7**, 2144 (1995).
(7) K. Yano, A. Usuki, A. Okada, T. Kurauchi, and O. Kamigaito, *J. Polym. Sci.: Part A: Polym. Chem.*, **31**, 2493 (1993).
(8) T. Lan, P. D. Kaviratna, and T. J. Pinnavaia, *Chem. Mater.*, **6**, 573 (1994).
(9) R. A. Vaia, S. Vasudevan, W. Krawiec, L. G. Scanlon, and E.P. Giannelis, *Adv. Mater.*, **7**, 154 (1995).
(10) E. P. Giannelis, *Adv. Mater.*, **8**, 29 (1996).
(11) P. B. Messersmith and E. P. Giannelis, *J. Polym. Sci.; Part A: Polym. Chem.*, **33**, 1047 (1995).
(12) L. Biasci, M. Aglietto, G. Ruggeri, and F. Ciardelli, *Polymer*, **35**, 3296 (1994).
(13) G. Oertel, *Polyurethane*, Kunststoff Handbuch, 3rd ed., Hanser, Munich, 1993.
(14) W. Meckel, W. Goyert, and W. Wieder, in *Thermoplastic Elastomers*, N. R. Legge, G. Holden, and H. E. Schroeder, Eds., Hanser, Munich, 1987.
(15) K. C. Frisch, *Rubber Chem. Tech.*, 126 (1980).
(16) A. J. Varma, M. D. Deshpande, and V. M. Nadkarni, *Angew. Makromol. Chem.*, **132**, 203 (1985).
(17) R. J. Janoski, US Patent 138562 (1995), assigned to Tremco, Inc.
(18) T. M. Garrett and I. Gruzins, US Patent 587038 (1997), assigned to MCP Industries, Inc.
(19) B. K. Kim, J. W. Seo, and H. M. Jeong, *Macromol. Res.*, **11**, 198 (2003).
(20) B. Finnigan, D. Martin, P. Halley, R. Truss, and K. Campbell, *Polymer*, **45**, 2249 (2004).
(21) P. Ni, J. Li, J. Suo, and S. Li, *J. Appl. Polym. Sci.*, **94**, 534 (2004).
(22) I. Rhoney, S. Brown, N. E. Hudson, and R. A. Pethrick, *J. Appl. Polym. Sci.*, **91**, 1335 (2004).
(23) X. Dai, J. Xu, X. Guo, Y. Lu, D. Shen, N. Zhao, X. Luo, and X. Zhang, *Macromolecules*, **37**, 5615 (2004).
(24) G. Gorrasi, M. Tortora, and N. Vittoria, *J. Polym. Sci.; Part B: Polym. Phys.*, **43**, 2454 (2005).
(25) W. J. Choi, S. H. Kim, Y. J. Kim, and S. C. Kim, *Polymer*, **45**, 6045 (2004).
(26) M. Song, D. J. Hourston, K. J. Yao, J. K. H. Tay, and M. A. Ansarifar, *J. Appl. Polym. Sci.*, **90**, 3239 (2003).
(27) A. Pattanayak and S. C. Jana, *Polymer*, **46**, 5183 (2005).
(28) H. M. Jeong, K. H. Jang, and K. Cho, *J. Macromol. Sci. B*, **B42**, 1249 (2003).
(29) B. K. Kim, J. W. Seo, and H. M. Jeong, *Eur. Polym. J.*, **39**, 85 (2003).
(30) H. C. Kuan, C.-C. M. Ma, W.-P. Chuang, and H.-Y. Su, *J. Polym. Sci.; Part B: Polym. Phys.*, **43**, 1 (2005).
(31) H. L. Tyan, Y. C. Liu, and K. H. Wei, *Chem. Mater.*, **11**, 1942 (1999).
(32) T.-K. Chen, Y.-I. Tien, and K.-H. Wei, *Polymer*, **41**, 1345 (2000).
(33) B. K. Kim and J. C. Lee, *J. Polym. Sci.; Part A: Polym. Chem.*, **34**, 1095 (1996).
(34) A. V. Richard, D. J. Klaus, J. K. Edward, and P. G. Emmanuel, *Chem. Mater.*, **8**, 2628 (1996).
(35) T. Agag, T. Koga, and T. Takeichi, *Polymer*, **42**, 3399 (2001).
(36) S.-Y. Moon, J.-K. Kim, C. Nah, and Y.-S. Lee, *Eur. Polym. J.*, **40**, 1615 (2004).
(37) T. Lan and T. J. Pinnavaia, *Chem. Mater.*, **6**, 2216 (1994).
(38) R. Krishnamoorti, R. A. Vaia, and E. P. Giannelis, *Chem. Mater.*, **8**, 1728 (1996).
(39) S.Abouzahr and G. L. Wilkes, *J. Appl. Polym. Sci.*, **29**, 2695 (1984).
(40) N. S. Schneider and C. S. Paik, *Polym. Eng. Sci.*, **17**, 73 (1977).
(41) S Subramani, Y. J. Park, I. W. Cheong, and J. H. Kim, *Polym. Int.*, **53**, 1145 (2004).
(42) T. Anagnostou and E. Jaul. *J. Coat. Tech.*, **53**, 35 (1981).
(43) J. H. Chang and Y. U. An, *J. Polym. Sci.; Part B: Polym. Phys.*, **40**, 670 (2002).
(44) Z. Wang and T. J. Pinnavaia, *Chem. Mater.*, **10**, 3769 (1998).